Shear flow induced polarization in ferroelectric smectics C

P. Pieranski, E. Guyon, P. Keller

Classification
Physics Abstracts
7.130 — 8.780

SHEAR FLOW INDUCED POLARIZATION IN FERROELECTRIC SMECTICS C

P. PIERANSKI, E. GUYON and P. KELLER (*)

Laboratoire de Physique des Solides, Université Paris-Sud, 91405 Orsay, France

(*Reçu le 11 avril 1975, accepté le 16 mai 1975*)

Résumé. — Des mesures récentes de polarisation en champ électrique [1] ont permis de démontrer l'existence de ferroélectricité dans des matériaux smectiques C chiraux. Dans cet article nous considérons le cas où la polarisation est produite par un cisaillement simple avec la vitesse parallèle aux couches smectiques : La structure hélicoïdale est modifiée par le cisaillement, et l'effet d'alignement donne naissance à un moment dipolaire résultant perpendiculaire au plan de cisaillement. L'étude de la dynamique de l'effet donne des informations sur l'élasticité et la viscosité mises en jeu dans cette distorsion. On discute aussi l'augmentation de polarisation près de la transition vers la phase smectique A.

Abstract. — The existence of ferroelectricity in the chiral smectic C phase has been established from polarization measurements in the presence of an electric field [1]. In this article we study the case where the polarization is created by applying a shear velocity parallel to the smectic planes : The helicoidal structure is distorted by the shear : The alignment effect induces the average dipoles in the smectic C planes to align perpendicular to the plane of the shear. The dynamics of the effect gives information on the elasticity and viscosity of the process. A significant increase of the polarization observed near the smectic A transition is discussed.

1. **Introduction.** — The existence of ferroelectric liquid crystals has been demonstrated recently [1]. The transverse electric dipoles **p** of chiral smectic C molecules tend to be aligned, in each smectic plane, along the same direction normal to the plane of tilt (see Fig. 1). This, in turn, can induce a spontaneous polarization **P** in each layer.

Because of the chirality of the molecules, the material itself behaves as a cholesteric : both the tilt direction and the polarization rotate from one layer to the next, as shown in figures 1*a* and *b*. The helicoidal structure can be distorted in a controlled way by external agents and several possible mechanisms are discussed in reference [1]. The application of a large electric field parallel to the layers has been shown experimentally to align the dipoles and to suppress the chirality of the structure [1, 2].

Another possibility, pointed out by L. Léger, comes from the aligning effect on the molecules by a shear flow. Figure 1*b* shows a top view of the undistorted helix. The polarization averaged over the sample thickness is zero when the thickness d is large enough ($\sim$ 200-600 μm) compared with the wavelength of the helix ($\lambda \sim 2\pi/q \sim$ several μm). A shear velocity $v_y(z)$ parallel to the layer distorts the helix configuration and induces a non-zero average polarization $\langle P_x \rangle$ in the perpendicular direction.

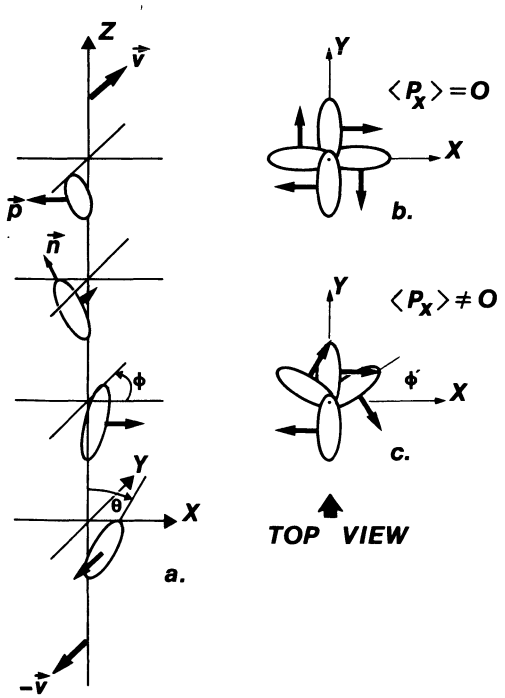

FIG. 1. — *a*) Representation of the chiral smectic C phase. The smectic layers are parallel to the xy plane. The molecules are tilted by an angle θ within the layers. The tilt plane rotates from one layer to the next. The angle φ describes this rotation. The electric dipole **p** is normal to the tilt plane. *b*) Top view of the unperturbed helix. Because of the axial symmetry, the average polarization vanishes. *c*) Due to the action of the shear along y, the axial symmetry of the configuration is broken and a non zero component of the average polarization appears along x.

(*) Aide partielle D.R.M.E., 74/556.

In this article, we discuss the ferroelectric behavior induced by such a shear.

The experiments were performed on the same material as those of reference [1] : -methyl-butyl-p-(p-decyloxybenzilidene amino) cinnamate. The formula of this chiral molecule is given in figure 2 together with the domains of existence of the different phases. The latent heat of the smectic A-smectic C transition is very small as compared with the other transitions. This is indicative of a nearly second order phase transition.

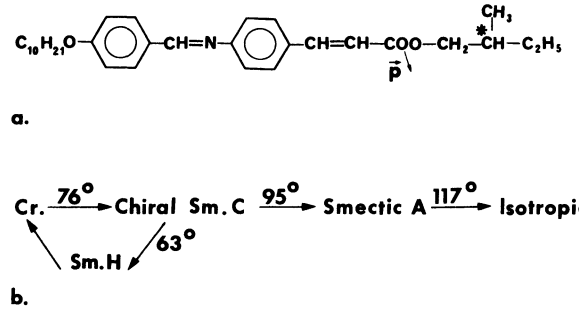

FIG. 2. — *a*) Structure of the chiral smectic C molecule. The effective transverse electric dipole **p** is localized on the COO group in the vicinity of the asymmetric carbon C*. *b*) Phase diagram of the material used. The smectic H phase can be attained only by cooling from the SmC phase. As explained in the text, the SmC-SmA transition is nearly second order.

The characterisation of the experimental set up plays a crucial role in the discussion of the results and will be discussed in section 2.

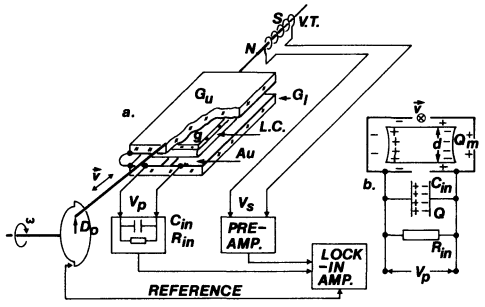

FIG. 3. — *a*) Experimental set-up. *b*) Equivalent electric circuit.

In section 3, we present experimental data demonstrating the existence of the shear flow induced polarization in the smectic C phase. The primary result is shown in figure 4. which gives the polarization as a function of temperature. The large signal increase around 94 °C is analysed in terms of a possible critical behavior near the second order transition to the smectic A phase.

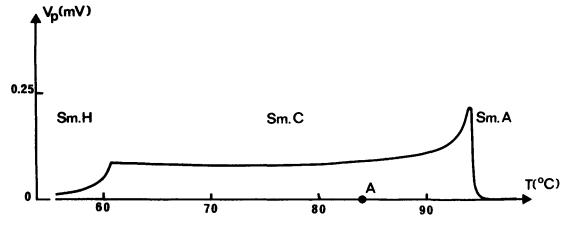

FIG. 4. — Plot of the shear flow induced voltage versus temperature.

In section 4, we develop a simplified theoretical model which can explain the experimental results. (In particular, it leads to a comparison with electric field determinations of the value of the transverse electric dipole **P** [1, 2]).

2. **Experimental.** — The flow cell is represented in figure 3*a*. The two horizontal glass plates G can slide relative to each other. The upper plate, G_u, moves with respect to the fixed lower one, G_l, with a sinewave velocity

$$v(t) = v_0 \, e^{j\omega t}$$

A solid bar connects the moving plate to a pin attached excentrically at a distance D_0 from the axis of a motor. The maximum available displacement and frequency are $2\,D_0 = 2$ cm and $\omega = 50\,\pi\,s^{-1}$.

The shear is measured with a velocity transducer (V. T. in figure 3*a*). A small magnet bar attached to the moving plate induces in a coil a voltage $V_S(t)$ proportional to the velocity $v(t)$. In the range of frequencies used, the phase shift between $v(t)$ and $V_S(t)$ is negligible.

The area of the sheared liquid crystalline film is precisely defined. A small glass plate g (18 × 5 mm) has been stuck under the upper plate G_u. The liquid crystal fills exactly the space under g and, due to capillarity effects, it remains localized there and does not leak into the rest of the cell.

The polarization charges are detected by means of two semi-transparent gold electrodes evaporated on G_l and G_u. These electrodes are isolated from the L.C. by a thin (0.1 mm) glass plate (not indicated on the figure 3*a*). The figure 3*b* shows schematically how the polarization is measured : the smectic layers are parallel to the glass plates due to surface induced alignment. When the shear is applied, polarization charges + and − Q_m develop on the lateral menisci of the liquid crystal. The gold electrodes provide two Faraday cages which can give a contactless measurement of the charges (the thickness d of the liquid crystal has been grossly exaggerated with respect to the width of the cell and the actual electrostatic influence between the cages is very small). Charges $\pm\,Q$, equal to $\pm\,Q_m$, are collected on the plates of an input capacitor (C_{in} = 21 650 pF). In the range of frequencies used, the impedance of this capacitor is much smaller than the preamplifier input FET's biasing resistor (R_{in} = 220 mΩ). Thus we can write that the measured voltage V_p equals Q_m/C_{in} and we can also neglect the phase lag between V_p and Q_m.

The charges $Q = Q_m$ represent the contribution of the polarization charges Q_p, remaining after the screening by the free ions. The characteristic time of this relaxation process is modified by the presence of the Faraday cages, which couple the sample electrically to the capacitor C_{in}. Therefore, the effective

capacitance of the sample is of the order of C_{in} whereas the effective internal resistance R_{eff} of the sample corresponds to the fraction ($\sim 1/10$) which is left uncovered by the electrodes. The evolution of the charges Q_m is described by the following equation :

$$\dot{Q}_m + \frac{1}{\tau} Q_m = \dot{Q}_p$$

where $\tau = R_{eff} C_{in}$.

This screening effect causes the phase of the charges Q_m to be in advance with respect to that of Q_p by an angle

$$\psi_1 = \tan^{-1} (1/\omega\tau) .$$

However, even for the lowest frequencies used, we have found that ψ_1 is very small and we can write $Q(t) = Q_m(t) = Q_p(t)$.

We have measured the RMS values of V_p and V_s, and the phase difference between them using a P.A.R.'s HR-8 Lock-in amplifier. The reference signal is delivered by an optical chopper driven by the motor axis.

The temperature of the sample is regulated electrically with a 0.1 °C accuracy. It is recorded by a small thermocouple in close contact with the glass plate. When optical controls were not performed, a thermally insulating box was set around the liquid crystal cell.

3. **Results.** — 3.1 OPTICAL CONTROL. — The interpretation of the results of conoscopic measurements is relatively simple and we discuss it first.

The alignment with the smectic planes parallel to the glass plates is obtained in the high temperature smectic A phase. The usual conoscopic image of an homeotropic material is seen (concentric rings and dark cross along the direction of the polarizers). The conoscopic image does not change, when the liquid crystal is sheared, up to the largest available shear rates ($\sim 300\ s^{-1}$). The result is consistent with the picture of smectics A with the smectic planes sliding easily over one another and where the molecules remain perpendicular to these planes. Upon cooling to the smectic C phase, the conoscopic image retains an axial symmetry. This result has been explained by Meyer and coworkers [1] as being due to the existence of the helix (see Fig. 1*a* and *b*) which keeps the average optical axis perpendicular to the layers (this result is valid in the limit of a small enough pitch. Here the pitch is of the order of several microns). When the shear flow is applied in the chiral smectic C phase, the conoscopic image is displaced in the direction of the flow. This fact is easy to understand if we assume that the helix is distorted as indicated on figure 1*c*. Far from the smectic A transition, the amplitude of the angular displacement of the conoscopic image is very small ($< 1°$). However, as the smectic A transition is approached, this displacement increases in a divergent manner.

There is one important complication in practice. In the presence of the shear, the buckling instabilities [6] disturb the conoscopic image. Thus , the measurement of the displacement angle is not very accurate and will not be used in the discussion.

3.2 TEMPERATURE DEPENDENCE OF THE POLARIZATION. — Experimentally, the buckling instability does not seem to affect the measurement of the shear flow induced polarization. Let us first consider the temperature dependence of the polarization effect. The velocity of the upper plate ($v_{RMS} = 7.58$ mm/s) and the frequency ($\omega = 10\ \pi\ s^{-1}$) are kept constant, while the temperature is allowed to drift slowly. Figure 4 gives a plot of the shear flow induced voltage V_p versus temperature. The curve starts to the right in the SmA phase and, far above the transition, no voltage is detected. As the SmA → SmC transition is approached, a voltage develops and this effect can be related to a pretransitional effect in the SmA phase [3]. We will not discuss this regime here since our temperature definition is not accurate enough across the sample to allow meaningful determinations of the critical behavior. On the other side of the transition, the voltage decreases with T. We will examine the possible causes of this behavior in the next section. Outside the transition region, the amplitude of the shear flow induced voltage V_p, as well as the phase shift between the excitation ($v(t)$ or $V_s(t)$) and $V_p(t)$, are nearly constant. At 61 °C, a SmC → SmH transition takes place. The voltage almost vanishes in the SmH phase and the phase lag angle ψ reaches 90°. Optically one observes a sudden increase of the density of disclinations. A quantitative discussion of the measurements in the Sm H phase shall not be attempted here. In an independent experiment we have used the racemic mixture (equal amounts of molecules of positive and negative chirality). This material *does not* exhibit any polarization effect in the smectic C phase, when sheared, as was predicted in reference [1].

3.3 SHEAR RATE DEPENDENCE. — Next, we consider the behavior at fixed temperatures. At a temperature $T_a = 84$ °C (Point A of figure 4) we studied the effect of variation of the frequency or of the amplitude of the shear. These two variations can be expressed in terms of the velocity of the moving plate. We have plotted, in figure 5, the dependence of the polarization voltage versus the average velocity v_{RMS} for both types of shear variation. At this temperature T_a, the phase lag ψ is very small for the frequencies used and increases with frequency. Typically, ψ reaches a value $\sim 5° \pm 1°$ at $\omega = 40\ \pi\ s^{-1}$.

4. **Theoretical.** — 4.1 DISTORTION. — In the present approach, we first calculate the distortion of the helix in the approximation of small perturbations, and, next, we obtain the average polarization in the direction transverse to the flow.

We base our discussion on the equations of nematodynamics [4]. If we assume that the flow does not change the tilt angle θ, the visco-elastic behavior of the

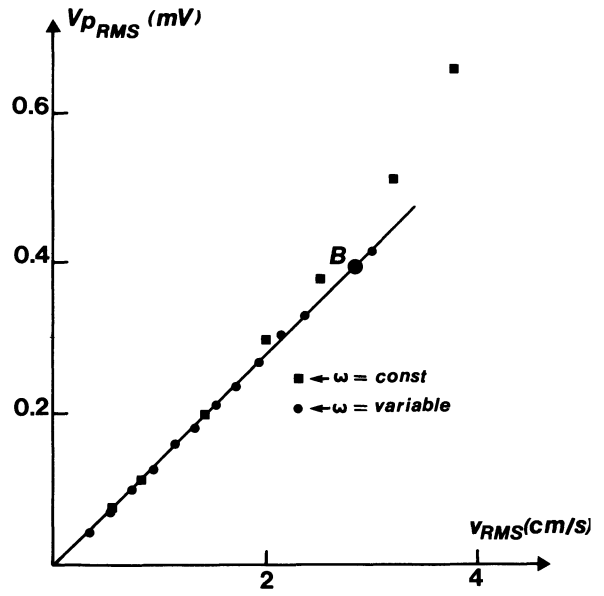

FIG. 5. — The shear flow induced voltage versus the shear rate.

smectic phase can be discussed as in the nematic one [5].

We neglect the perturbation of the flow caused by the helical ordering. In other words, the velocity field which satisfies the Leslie equations of motion is approximated by a simple shear flow, characterized by the shear rate v/d. With this simplification, we have only one equation of motion (for the director) to solve. The director has only one degree of freedom, namely the rotation around the z axis, described by the variable φ (Fig. 1). Thus, we consider only the equation of equilibrium of the z component of the acting torques :

$$(K_3 \sin^2\theta\cos^2\theta + K_2 \sin^4\theta)\frac{d^2\varphi}{dz^2} - \gamma_1 \sin^2\theta\dot{\varphi} = $$

$$= -\sin\theta\cos\theta\alpha_2\cos\varphi\frac{v}{d}. \quad (1)$$

The left hand side terms correspond to the elastic and viscous torques, which both oppose the deformation of the helix. The right hand side represents the perturbing action of the shear flow.

Two terms contribute to the expression for the elastic torques ; the bend (K_3) and the tilt (K_2) distortion. In the range of tilt angles values θ obtained (0°-20°) [2] the bend term is dominant ; in the following we neglect the twist term.

In the approximation of small perturbations, the destabilizing torque $\Gamma \cong \alpha(\theta).\frac{v}{d}e^{i\omega t}\cos qz$ will excite only the perturbation modes of the same spatial and time period. This assumption is confirmed by a direct observation on an oscilloscope of the shear flow induced voltage. It is a sinusoidal function of time with the same frequency as the shear. The helix configuration distorted by the flow can be written as

$$\varphi(z, t) = \varphi_s(z) + \varphi'(z, t) \quad (2)$$

where φ_s stays for the unperturbed configuration ; $\varphi_s = qz$, and $\varphi' = \varphi_0 e^{j(\omega t+\psi)}\cos qz$ is the small distortion (defined in figure 1c) caused by the flow alignment effect. Introducing this expression in eq. (1), we obtain

$$(j\omega\gamma_1 + K_3 q^2)\varphi_0 e^{j\psi} = \frac{1}{\operatorname{tg}\theta}\alpha_2\frac{v_0}{d} \quad (3)$$

which leads to the following expression for the amplitude and phase shift of the distortion

$$\varphi_0 = \frac{1}{\operatorname{tg}\theta}\frac{\alpha_2}{\gamma_1}\frac{1}{\sqrt{\omega^2 + \frac{1}{\tau^2}}}\frac{v_0}{d} \quad (4)$$

$$\psi = -\tan^{-1}(\omega\tau) \quad (5)$$

where

$$\tau = \frac{\gamma_1}{K_3 q^2}$$

is a characteristic time constant for the spontaneous relaxation of the distortion ([1]).

4.2 ELECTRIC POLARIZATION. — In the present experiment we measured the surface charge density $\sigma = Q/l.d$, where l is the length of the meniscus along the shear direction. σ is equal to the x-component of the average polarization density in the sample $\sigma = \langle P_x \rangle$. As can be seen from figure 1c, the x-component of the polarization density is $P.\sin\varphi$. Its average value, calculated in the presence of the shear flow induced distortion, is :

$$\langle P_x \rangle = \langle P.\sin\varphi \rangle \simeq \tfrac{1}{2} P.\varphi_0.e^{j(\omega t+\psi)} \quad (6)$$

where φ_0 is given by form [4].

4.3 NUMERICAL ESTIMATES. — Let us analyze our results in view of a possible determination of P. For a particular experimental point B on figure 5a, we measured $V_{p(RMS)} = 390$ μV. Consequently, the polarization charge per unit length is :

$$\frac{Q}{l} = \frac{C_{in} \times V_{PRMS} \times \sqrt{2}}{l} = 0.66 \times 10^{-9}\ \text{C/m}. \quad (7)$$

Another determination of this ratio

$$Q/l = \sigma.d = \langle P_x \rangle.d$$

can be obtained using formulas (5) and (6)

$$\frac{Q}{l} = \frac{1}{2}\frac{\alpha_2}{\gamma_1}.\frac{1}{\sqrt{\omega^2 + 1/\tau^2}}.\frac{1}{\operatorname{tg}\theta}.v_0.P.f(\theta). \quad (8)$$

([1]) *Note* : In the MPP [5] formulation of the hydrodynamics of smectic C phase (form 4.5) the numerical coefficient λ [1] corresponds to α_2/γ_1. Similarly, our elasticity coefficient

$$(K_3 \sin^2\theta\cos^2\theta + K_2 \sin^4\theta)$$

corresponds to B_3 of reference [4] (form 7.61).

If we assume that the polarization depends linearly on the tilt angle θ, we approximate $f(\theta)/\text{tg}\,\theta$ by eq. (1).

In nematics, α_2/γ_1 is of the order of unity. For the moment, we assume that this estimate is valid also in the SmC phase.

An independent estimate of P can be obtained from electric polarization measurements [2] which give a value of the electric dipole moment $P \sim 0.02$ D/molecule, which leads to the polarisation density

$$P \simeq 3.84 \times 10^{-4} \frac{C}{m^2}.$$

Finally, from the phase lag angle determination $\psi = 5°$ at $\omega = 40\ s^{-1}$ (see form (5)), we calculate $\tau = 7 \times 10^{-4}$ s.

Using these different estimates, we deduce a value $Q/l = 5.4 \times 10^{-9}$ C/m which is larger by a factor 8 than the measured value $Q/l = 0.66 \times 10^{-9}$ C/m. A possible reason for this disagreement is the choice we have made of the α_2/γ_1 value. In smectics, γ_1 should depend essentially on the interactions in the smectic layers, while α_2 is conditioned by interlayer interactions. Consequently, α_2/γ_1 could be smaller than 1.

4.4 QUALITATIVE AGREEMENT. — From the qualitative point of view, the formula (8) can explain the characteristics of the dependence of the polarisation on the shear rate.

If we keep the frequency constant and vary the shear rate by changing the amplitude of the motion, the linear behavior observed on figure 5 is in agreement with the formula (8).

If the amplitude is constant, and the frequency varies, the dependence of the polarization on frequency predicted by this formula is $\frac{\omega}{\sqrt{\omega^2 + 1/\tau^2}}$.

If we assume that τ is of the order of 10^{-3} s, this dependence is also nearly linear in the range of frequencies used. The experimental observations confirm this result.

4.5 PRETRANSITIONAL BEHAVIOR. — We come back to the relatively singular behavior near the

$$\text{SmC} \rightarrow \text{SmA}$$

transition (see Fig. 3*a*) which is nearly second order. Recent X-ray measurements [2] show that the tilt angle goes progressively to zero at T_c as :

$$\theta \propto (T_c - T)^{\beta} \quad \text{with} \quad \beta = 0.35 \pm 0.05.$$

1) In our naive approach based on a nematic-like equation for the director, the shear flow polarization response function (eq. (4) (6)) is not expected to diverge near T_c. In formula (8), tg θ goes to zero as θ but the polarization introduces a new factor $f(\theta)$ vanishing linearly with θ and the two effects should cancel out. This gives rise to a finite polarization at T_c as obtained experimentally. Several paths can be explored concerning the increase of polarization near T_c and we just mention their possibility.

2) The approach sketched above assumes that the dynamic coefficients are regular (Van Hove hypothesis) as they should depend on microscopic interactions even near the transition. That is to say, the singular behavior comes only from divergence of static parameters. In smectics A it has been shown from a mode-mode coupling description that such an assumption is not sufficient. A singular contribution in any of the three terms α_2, γ_1, K_3 can modify the behavior near T_c. However, a mode-mode coupling analysis ([2]) does not seem to indicate such a singular behavior in the smectic C phase.

3) We observed that, in large shears and near T_c, the *monocrystalline* smectic C structure is broken. In very small samples where the thermal gradients effects were minimized, this rupture could cause an abnormal and sudden increase of the polarization. In the results shown on figure 4, this instability has not taken place.

4) Near the A-C transition the shear can induce changes in the tilt angle θ [7, 8]. In the high temperature phase, this could lead to a diverging polarization at T_c. Similarly one could expect this effect to cause a divergence when T_c is approached from below. However, this effect would affect only the critical behavior very near T_c with a temperature resolution not attained in the present experiments.

5) The broad range of variation of P in figure 4 suggests another explanation based on variations of the pitch $2\pi/q$ with temperature. At low frequencies, the response function (eq. (4)) is proportional to the time $\tau = \gamma_1/Kq^2$ when T increases. In the smectic C domain, the pitch of the cholesteric helix is known to increase by a factor of 3[2]. This variation could explain part of the increase of the phase lag angle and consequently of the response function.

Acknowledgments. — This work has benefited from many interactions and it is a pleasure to acknowledge some crucial ones : R. B. Meyer for a first introduction to the problem, L. Liébert and L. Strzelecki for their chemical skills without which this work would have not existed, M. Lambert for discussions on the ferroelectric problems, P. G. de Gennes, G. Toulouse and F. Brochard on the critical behavior at the smectic C-smectic A transition, G. Durand, Ph. Martinot-Lagarde and R. Duke for many suggestions and communications of results of unpublished work on chiral smectic C.

([2]) Brochard, F., Private communication.

References

[1] MEYER, R. B., LIÉBERT, L., STRZELECKI, L. and KELLER, P., *J. Physique Lett.* **36** (1975) L-69.

[2] DUKE, R., DURAND, G., KELLER, P., LIÉBERT, L. and MEYER, R. B., to be published in *J. Physique*.

[3] RIBOTTA, R., MEYER, R. B. and DURAND, G., *J. Physique Lett.* **35** (1974) L-161.

[4] DE GENNES, P. G., *The Physics of Liquid Crystals*, (Clarendon Press Oxford) 1974.

[5] MARTIN, P., PARODI, O. and PERSHAN, P. S., *Phys. Rev.* **6** (1972) 2401.

[6] DELAYE, M., RIBOTTA, R. and DURAND, G., *Phys. Lett.* **44** A (1973) 139.

[7] This point was raised to us by the referee.

[8] BROCHARD, F., Thèse Orsay (1975), chap. III.